2013 IEEE International Conference on Systems, Man, and Cybernetics

Direct Adaptive Fuzzy-Wavelet-Neural-Network Control for Electric Two-Wheeled Robotic Vehicles

Ching-Chih Tsai
Department of Electrical Engineering
National Chung Hsing University
Taichung, Taiwan
Email:cctsai@nchu.edu.tw

Ching-Hang Tsai
Department of Electrical Engineering
National Chung Hsing University
Taichung, Taiwan
Email:kiddanike159753@hotmail.com

***Abstract*—This paper presents a direct adaptive motion controller using fuzzy wavelet neural networks (FWNN) for speed control of an electric two-wheeled robotic vehicle (ETWRV) with unknown parameters and uncertainties. With the decomposition of the overall system into two subsystems: yaw motion control and mobile inverted pendulum, two direct adaptive FWNN motion controllers are respectively proposed to achieve station keeping, speed following and yaw motion control. Asymptotic stabilities of the two controllers with their FWNN weighting updating rules are derived via the Lyapunov stability theory. Simulation results indicate that the proposed controllers are capable of providing satisfactory control actions to steer the vehicle.**

***Keywords*—Adaptive control, fuzzy wavelet neural networks (FWNN), posture and speed control, two-wheeled robotic vehicle, yaw motion.**

I. INTRODUCTION

Recently, electric two-wheeled robotic vehicles (ETWRV), similar to Segway^{TM}, have been well recognized as powerful personal transportation vehicles. Such vehicles can be usually constructed by a synthesis of mechatronics, control techniques and software. Unlike Segway^{TM} where the riders must stand on it, researchers in [1]-[2] presented two-wheeled robotic vehicles to let the driver have a comfort seat while driving, and claimed that the vehicles could become prevalent two-wheeled human transporters, thus satisfying human requirements of convenient and low-cost short-distance transportation.

Many researchers have designed and implemented Segway^{T}-like two-wheeled robotic vehicles. Tsai *et al.* [3] proposed an adaptive neural network control of a self-balancing two-wheeled scooter. Pathak *et al.* [4] studied the dynamic equations and control of the wheeled inverted pendulum by partial feedback linearization. Furthermore, several researchers in [5]-[8] have proposed useful control techniques for various two-wheeled vehicles or inverted-pendulum-type vehicles. As authors' best understanding, the adaptive direct control problem of self balancing, speed tracking and yaw rate control problems deserves more investigations on improving control performance of the two-wheeled robotic vehicles.

Recently, fuzzy-basis-function networks (FBFNs) have been adopted widely for nonlinear system modeling and control because they possess simple structure, good local approximating performance, particular resolvability, and function equivalence to a class of nonlinear function. Hence, FBFNs are increasingly receiving attention in solving complex and practical problems. For example, Lin and Wang [9] presented FBFN-based robust self-tuning controller for robotic arms, Huaguang *et al.* [10] investigated an FBFN-based multivariable adaptive controller for nonlinear systems, Lin [11] proposed an adaptive critic controller using FBFN for bank-to-turn missiles. Furthermore, Tsai *et al.* [12] employed two FBFNs to approximate the modeling errors, unknown Coulomb and static frictions occurring in a two-wheeled self-balancing human transporter.

Fuzzy wavelet networks (FWNN) have been proved to excellently approximate time-varying nonlinear functions or nonlinear dynamics [13]. This property can be easily applied to controller design. For example, Lin [14] brilliantly used FWNN to on-line learn a nonsingular terminal sliding mode controllers for robot manipulators, thus accomplishing out excellent trajectory tracking performance. Tsai *et al.* [15] presented the use of FWNN together with nonsingular terminal sliding control method to control Mecanum wheeled omnidirectional vehicles. However, the FWNN method in [14,15] has not yet been applied to two-wheeled robotic vehicles by addressing the self balancing, speed tracking and yaw rate problem for this kind of transporter.

The objective of this paper is to develop a direct adaptive FWNN-based motion control approach for posture maintenance, speed following and yaw motion control of ETWRV with unknown parameters and uncertainties. The contributions of the paper are threefold. First, with the help of the decoupling transformation matrix in [16] a direct adaptive FWNN yaw motion controller and a direct adaptive FWNN posture and speed controller are independently designed using a nonlinear, decoupling model of the ETWRV, in order to achieve posture maintenance, speed and yaw motion control. Second, the proposed motion controllers are proven asymptotically stable using Lyapunov stability theory. Third, the proposed controllers are shown effective for the ETWRV with unknown parameters and uncertainties.

The rest of the paper is outlined as follows. Section II briefly describes the nonlinear modeling and system decomposition of the robot and the FWNN. Section III and IV respectively develop both direct adaptive FWNN-based yaw motion and speed controllers for posture and speed

978-1-4799-0652-9/13 $31.00 © 2013 IEEE
DOI 10.1109/SMC.2013.432

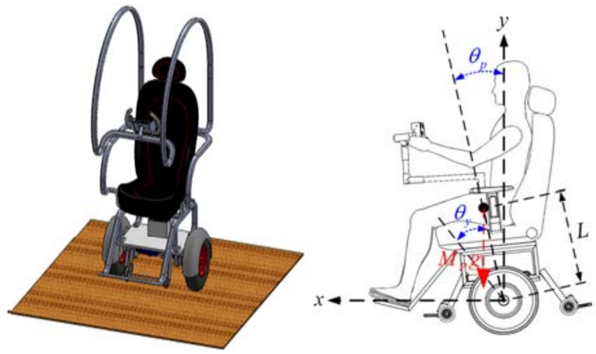

(a) (b)

Fig.1. (a) Physical structure of the ETWRV; (b) illustration of defined symbols.

control, and yaw motion control, respectively. In Section V computer simulations are conducted to show the feasibility and effectiveness of both proposed controllers. Section VI concludes the paper.

II. PRELIMINARIES

A. Nonlinear Mathematical Modeling

To steer the robot, mathematical model is necessary such that the robot with the designed controllers can successfully achieve desired control objectives. Fig. 1 depicts the free body diagram of the ETWRV, and Table I lists all the used symbols and their definitions. The nonlinear system model of the robot is modified from [3,12,16] and described in the following state-space form.

$$\dot{v}_{RM} = A_{22}v_{RM} + A_{23}\sin\theta_P + B_2(C_L + C_R) + B_{23}f_{dRL} + B_{24}f_{dRR} + B_{25}f_{dP} \tag{1}$$

$$\dot{\omega}_P = A_{43}\sin\theta_p + B_4C_L + B_4C_R + B_{45}f_{dp}, \tag{2}$$

$$\dot{\omega}_y = A_{66}\omega_y + B_{61}C_L + B_{62}C_R + B_{63}f_{dRL} + B_{64}f_{dRR}. \tag{3}$$

where the parameters in (1-3) are given in [12].Moreover, the nonlinear state equations (1-3) can be rewritten in the following state-space form

$$\begin{bmatrix} \dot{x}_{RM} \\ \dot{v}_{RM} \\ \dot{\theta}_p \\ \dot{\omega}_p \\ \dot{\theta}_y \\ \dot{\omega}_y \end{bmatrix} = \begin{bmatrix} v_{RM} \\ A_{22}v_{RM} + A_{23}\sin\theta_p \\ \omega_p \\ A_{43}\sin\theta_p \\ \omega_y \\ A_{66}\omega_y \end{bmatrix} + \begin{bmatrix} 0 & 0 \\ B_2 & B_2 \\ 0 & 0 \\ B_4 & B_4 \\ 0 & 0 \\ B_6 & -B_6 \end{bmatrix} \begin{bmatrix} C_L \\ C_R \end{bmatrix} + \begin{bmatrix} 0 \\ f_2 \\ 0 \\ f_4 \\ 0 \\ f_6 \end{bmatrix} \tag{4}$$

where

$$f_2 = B_{23}f_{dRL} + B_{24}f_{dRR} + B_{25}f_{dP},\ f_4 = B_{45}f_{dP},\ f_6 = B_{63}f_{dRL} + B_{64}f_{dRR} \tag{5}$$

From (4), if there are no uncertainties and the vehicle has reached a steady-state inclination θ_p, i.e., $\dot{\theta}_p = 0$, then it will generate a steady-state linear speed expressed by

$$v_{SS} = \frac{B_2A_{43} - A_{23}B_4}{A_{22}B_4}\sin\theta_p \Big|_{\dot{\theta}_p = 0}. \tag{4}$$

This steady-state linear speed intends to move the robot without falling down according to the tilt angle. With the use

Table I. Symbols Definition

Symbol and unit	Parameter and variable name	Values
x_{RM} [m], v_{RM} [m/s]	position, speed	—
θ_P [rad], ω_P [rad/s]	pitch angle, pitch angle rate	—
θ_y [rad], ω_y [rad/s]	yaw angle, yaw angle rate	—
C_L [$N\cdot m$]	applied torque on left wheel	—
C_R [$N\cdot m$]	applied torque on right wheel	—
J_{RR} [$kg\cdot m^2$], J_{RL} [$kg\cdot m^2$]	Moment of inertia of the rotation mass with respect to the z axis	0.11kg.m^2
M_{RR} [kg], M_{RL} [kg]	Mass of the rotation mass connected to the left and right wheel	—
$J_{P\theta}$ [$kg\cdot m^2$]	Moment of inertia of the chassis with respect to the z axis	27.6kg.m^2
$J_{P\delta}$ [$kg\cdot m^2$]	Moment of inertia of the chassis with respect to the y axis	3.478kg.m^2
M_P [kg]	Mass of the chassis	135kg
R [m]	Radius of the wheels	0.2m
D [m]	Lateral distance between the contact patches of the wheels	0.6m
L [m]	Distance between the z axis and the CG of the chassis	1m
b	Friction coefficient	0.01~0.05

of the transformation of the torques C_y and C_θ into the wheel torques C_L and C_R

$$\begin{bmatrix} C_L \\ C_R \end{bmatrix} = \begin{bmatrix} 0.5 & 0.5 \\ 0.5 & -0.5 \end{bmatrix} \begin{bmatrix} C_\theta \\ C_y \end{bmatrix}. \tag{5}$$

With (7), (5) becomes

$$\begin{bmatrix} \dot{x} \\ \dot{v} \\ \dot{\theta}_p \\ \dot{\omega}_p \\ \dot{\theta}_y \\ \dot{\omega}_y \end{bmatrix} = \begin{bmatrix} v \\ A_{22}v + A_{23}\sin\theta_p \\ \omega_p \\ A_{43}\sin\theta_p \\ \omega_y \\ A_{66}\omega_y \end{bmatrix} + \begin{bmatrix} 0 & 0 \\ B_2 & B_2 \\ 0 & 0 \\ B_4 & B_4 \\ 0 & 0 \\ B_6 & -B_6 \end{bmatrix} \begin{bmatrix} C_L \\ C_R \end{bmatrix} + \begin{bmatrix} 0 \\ f_2 \\ 0 \\ f_4 \\ 0 \\ f_6 \end{bmatrix}. \tag{6}$$

Observing (6) reveals that there are two independent subsystems: one is concerned with the mobile inverted pendulum subsystem regarding self-balancing of the platform, i.e., for $B_2 < 0$ and $B_4 < 0$.

$$\begin{bmatrix} \dot{x} \\ \dot{v} \\ \dot{\theta}_p \\ \dot{\omega}_p \end{bmatrix} = \begin{bmatrix} v \\ A_{22}v + A_{23}\sin\theta_p \\ \omega_p \\ A_{43}\sin\theta_p \end{bmatrix} + \begin{bmatrix} 0 \\ B_2 \\ 0 \\ B_4 \end{bmatrix} C_\theta + \begin{bmatrix} 0 \\ f_2 \\ 0 \\ f_4 \end{bmatrix} \tag{7}$$

and the other is the yaw motion system model regarding the yaw motion, i.e.,

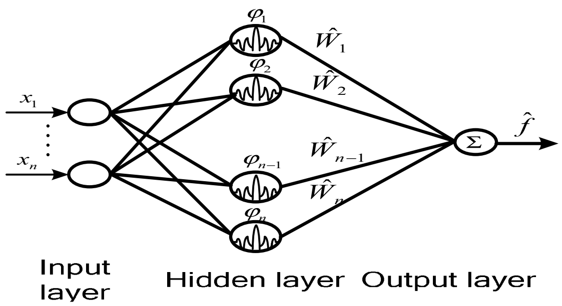

Fig.2. FWNN structure.

$$\begin{bmatrix}\dot{\theta}_y\\ \dot{\omega}_y\end{bmatrix}=\begin{bmatrix}0 & 1\\ 0 & A_{66}\end{bmatrix}\begin{bmatrix}\theta_y\\ \omega_y\end{bmatrix}+\begin{bmatrix}0\\ B_6\end{bmatrix}(C_y+\bar{f}_6),\ \bar{f}_6=f_6/B_6, B_6>0 \quad (8)$$

From (7) and(8), it indicates that two controllers for C_θ and C_y can be synthesized independently from each other and then combined together to accomplish the control goal.

B. Fuzzy Wavelet Neural Networks (*FWNN*)

The FWNN performs excellent approximations for the curve fitting problems and it can be trained to learn some classes of nonlinear functions and system dynamics easily and quickly. The approximation accuracy and convergent rate of the FWNN may be further improved with a strategy for selecting appropriate centers and widths of the receptive fields. Fig. 2 depicts the structure of the FWNN whose outputs can be given by , for $k=1,\cdots,m$,

$$\hat{f}=\sum_{j=1}^{N}W_k\varphi_j(\boldsymbol{x}) \quad \text{, or } \mathbf{f(x,c,\omega,W)}=\mathbf{W^T\varphi(x,c,\omega)} \quad (9)$$

where

$\varphi_j(\boldsymbol{x})=\varphi_j(x_1)\cdots\varphi_j(x_n)$,

$\varphi_j(x_i)=[1-\omega_{ji}{}^2(x_i-c_{ji})^2]e^{\{-\omega_{ji}{}^2(x_i-c_{ji})^2\}}$

$\boldsymbol{x}=\left[x_1,x_2,...,x_n\right]^T\in\mathbb{R}^n.\boldsymbol{c}=\left[c_1^T,c_2^T,...,c_N^T\right]^T\in\mathbb{R}^{n\times N}$,

$\boldsymbol{\omega}=\left[\omega_1^T,\omega_2^T,...,\omega_N^T\right]^T\in\mathbb{R}^{n\times N},\mathbf{c}_j=\left[c_{j1},c_{j2},...,c_{jn}\right]^T\in\mathbb{R}^n$,

$\boldsymbol{\omega}_j=\left[\omega_{j1},\omega_{j2},...,\omega_{jn}\right]^T\in\mathbb{R}^n,\mathbf{W}^T=\left[W_k\right]^T$ is an $1\times N$ matrix and $\boldsymbol{\varphi}(\mathbf{x},\mathbf{c},\boldsymbol{\omega})=\left[\varphi_1(x)\quad\varphi_2(x)\quad\cdots\quad\varphi_N(x)\right]^T$.

By the Stone–Weierstrass theorem, the FWNNN can be proved that it is capable of uniformly approximating any real continuous function $f(x)$ on a compact set $\mathbf{U}$ to any arbitrary accuracy b_ε [21], i.e., there exists an ideal FWNN, $\boldsymbol{W^T S(x,c,\omega)}$, with ideal parameters, $\mathbf{c},\boldsymbol{\omega},\text{and}\,W$ such that $\sup_{x\in\mathbf{U}}\left\|f(x)-\mathbf{W}^T\boldsymbol{\varphi}(\mathbf{x},\mathbf{c},\boldsymbol{\omega})\right\|<b_\varepsilon$. Therefore, $f(x)$ can be represented as

$$f(x)=\mathbf{W}^T\boldsymbol{\varphi}(\mathbf{x},\mathbf{c},\boldsymbol{\omega})+\varepsilon_f \quad (10)$$

where $\left\|\varepsilon_f\right\|\le b_\varepsilon$. In this paper, all norms of vectors and matrices adopt Frobenius norm. The norms of the ideal parameters should satisfy the following assumption.

Assumption 1: The norms of ideal parameters, $\|c\|,\|\omega\|,and\|W\|$, are bounded by positive real values, i.e. $\|c\|\le b_c,\|\omega\|\le b_\omega,and\|W\|\le b_W$ .Clearly, we need to estimate the ideal FWNN by an estimate FWNN $\hat{f}(x)=\hat{W}^T\boldsymbol{\varphi}(\mathbf{x},\hat{\mathbf{c}},\hat{\boldsymbol{\omega}})$. The weight updating law will be stated in the following section.

III. FWNN YAW MOTION CONTROLLER DESIGN

This section is devoted to constructing an adaptive sliding-mode yaw controller for the subsystem (8) with the two parameters, A_{66} and B_6 , and the unknown nonlinear term $\bar{f}_6$. Since the potentiometer is employed to measure the angle difference between the desired yaw angle and the actual yaw angle that the rider intended to achieve, the direct adaptive FWNN yaw control problem is reduced to an adaptive regulation problem. In what follows, the backstepping technique is used to attain this adaptive yaw motion controller by choosing the virtual control $\omega_y=-K_y\theta_y$ and the Lyapunov function $V=\theta_y{}^2/2$, and then stabilizing the θ_y - dynamics. Next, define the second backstepping error as the sliding surface s_y

$$s_y=\xi_y=\omega_y+K_y\theta_y=\dot{\theta}_y+K_y\theta_{y.} \quad (11)$$

Differentiating s_y gives

$$\begin{aligned}\dot{s}_y=\dot{\xi}_y=\dot{\omega}_y+K_y\dot{\theta}_y&=\left[A_{66}\omega_y+B_6(C_y+\bar{f}_6)\right]+K_y\omega_y\\&=\left(K_y+A_{66}\right)\omega_y+B_6(C_y+\bar{f}_6)\\&=B_6\left[\left(\frac{K_y+A_{66}}{B_6}\right)\omega_y+(C_y+\bar{f}_6)\right]=B_6(C_y+\bar{\bar{f}}_6)\end{aligned} \quad (12)$$

where $\bar{\bar{f}}_6=\left(\dfrac{K_y+A_{66}}{B_6}\right)\omega_y+\bar{f}_6)$. In order to stabilize this yaw control subsystem, this subsection proposes the following control law;

$$C_y=-\hat{\bar{\bar{f}}}_6-\left(k_1+\hat{g}_{y\max}\right)\mathrm{sgn}(s_y)-k_2s_y,\ \ k_1>0,k_2>0$$

(13)

$\hat{\bar{\bar{f}}}_6$ is the estimate of $\bar{\bar{f}}_6$ by using the FWNN proposed in Section II.B, namely that

$$\bar{\bar{f}}_6=W_y^{*T}\varphi^*{}_y+\varepsilon_y{}^*=[W_{1y}{}^*\cdots W_{ny}{}^*][\varphi^*{}_{y1}\quad\cdots\quad\varphi^*{}_{yn}]^{\mathrm{T}}+\varepsilon_y{}^*$$

(14)

and

$$\hat{\bar{\bar{f}}}_6=\hat{W}_y{}^T\hat{\varphi}_y=[\hat{W}_{1y}\cdots\hat{W}_{ny}][\hat{\varphi}_{1y}\quad\cdots\quad\hat{\varphi}_{ny}]^{\mathrm{T}} \quad (15)$$

where

$$\begin{aligned}\varphi^*{}_{yi}&=\left\{1-\left(\theta_y-c^*{}_{1yi}\right)^2\omega^*{}_{1yi}{}^2\right\}\left\{1-\left(\omega_y-c^*{}_{2yi}\right)^2\omega^*{}_{2yi}{}^2\right\}\\&\quad*\exp\left\{-[\left(\theta_y-c^*{}_{1yi}\right)^2\omega^*{}_{1yi}{}^2+\left(\omega_y-c^*{}_{2yi}\right)^2\omega^*{}_{2yi}{}^2]\right\}\end{aligned} \quad (16)$$

and

$$\hat{\varphi}_{yi} = \left\{1-\left(\theta_y - \hat{c}_{1yi}\right)^2 \hat{\omega}_{1yi}{}^2\right\}\left\{1-\left(\omega_y - \hat{c}_{2yi}\right)^2 \hat{\omega}_{2yi}{}^2\right\}$$
$$*\exp\left\{-[\left(\theta_y - \hat{c}_{1yi}\right)^2 \hat{\omega}_{1yi}{}^2 + \left(\omega_y - \hat{c}_{2yi}\right)^2 \hat{\omega}_{2yi}{}^2]\right\} \tag{17}$$

Moreover, by defining $\tilde{W}_y = W_y{}^* - \hat{W}_y$, $\tilde{\varphi}_y = \varphi^*{}_y - \hat{\varphi}_y$, one obtains

$$\bar{\bar{f}}_6 = W_y^{*T}\varphi_y^* + \varepsilon_y^* = \hat{W}_y^T\hat{\varphi}_y + \hat{W}_y^T\tilde{\varphi}_y + \tilde{W}_y^T\hat{\varphi}_y + \tilde{W}_y^T\tilde{\varphi}_y + \varepsilon_y^* \tag{18}$$

In order to achieve on-line tuning of the FWNN parameters, including the center vector $c = [c_{11}\ c_{21}\ c_{31}\ ...\ c_{1n}\ c_{2n}\ c_{3n}]^T$ and the vector $\omega = [\omega_1\ \omega_2\ \omega_3\ ...\ \omega_n]^T$, the expansion of $\tilde{\varphi}$ is taken in a Taylor series as follows.

$$\tilde{\varphi}_y = \frac{\partial\tilde{\varphi}_y}{\partial\hat{c}_y}\tilde{c}_y + \frac{\partial\tilde{\varphi}_y}{\partial\hat{\omega}_y}\tilde{\omega}_y + h_y = \bar{A}_y\tilde{c}_y + \bar{B}_y\tilde{\omega}_y + h_y \tag{19}$$

where $\tilde{c}_y = c_y{}^* - \hat{c}_y$; $\tilde{\omega}_y = \omega_y^* - \hat{\omega}_y$; h_y is the vector containing higher order terms and satisfies $\|h_y\| \le b_y$. Substituting (19) into (18) gives

$$\bar{\bar{f}}_6 = \hat{W}_y{}^T\hat{\varphi}_y + \hat{W}_y{}^T(\bar{A}_y\tilde{c}_y + \bar{B}_y\tilde{\omega}_y) + \tilde{W}_y{}^T\hat{\varphi}_y + \varepsilon_y \tag{20}$$

Where $\varepsilon_y = \tilde{W}_y{}^T h_y + \tilde{W}_y{}^T\tilde{\varphi}_y + \varepsilon_y^*$ and ε_y is assumed to satisfies $|\varepsilon_y| < g_{y\max}$.

Substituting the control law (13) into (12) gives

$$\begin{aligned} \dot{s}_y &= B_6(-\hat{\bar{f}}_6 - \left(k_1 + \hat{g}_{y\max}\right)\mathrm{sgn}(s_y) - k_2 s_y + \bar{\bar{f}}_6) \\ &= B_6(\hat{W}_y^T(\bar{A}_y\tilde{c}_y + \bar{B}_y\tilde{\omega}_y) + \tilde{W}_y^T\hat{\varphi}_y + \varepsilon_y - \left(k_1 + \hat{g}_{y\max}\right)\mathrm{sgn}(s_y) - k_2 s_y) \end{aligned} \tag{21}$$

and

$$\begin{aligned} s_y\dot{s}_y &= B_6 s_y(\hat{W}_y^T(\bar{A}_y\tilde{c}_y + \bar{B}_y\tilde{\omega}_y) + \tilde{W}_y^T\hat{\varphi}_y + \varepsilon_y - \left(k_1 + \hat{g}_{y\max}\right)\mathrm{sgn}(s_y) - k_2 s_y) \\ &\le B_6(\hat{W}_y^T(\bar{A}_y\tilde{c}_y + \bar{B}_y\tilde{\omega}_y) + \tilde{W}_y^T\hat{\varphi}_y)s_y + B_6(g_{y\max} - \hat{g}_{y\max})|s_y| - B_6(k_2|s_y| + k_2 s_y{}^2) \\ &= B_6(\hat{W}_y^T(\bar{A}_y\tilde{c}_y + \bar{B}_y\tilde{\omega}_y) + \tilde{W}_y^T\hat{\varphi}_y)s_y + B_6\tilde{g}_{y\max}|s_y| - B_6(k_2|s_y| + k_2 s_y{}^2) \end{aligned} \tag{22}$$

where $\tilde{g}_{y\max} = g_{y\max} - \hat{g}_{y\max}$ Moreover, the subsequent Lyapunov function candidate is employed to find the parameter updating laws of $\dot{\hat{\mathbf{W}}}_y$, $\dot{\hat{\mathbf{c}}}_y$, and $\dot{\hat{\boldsymbol{\omega}}}_y$, $\dot{\hat{g}}_{y\max}$.

$$\begin{aligned} V_1 &= s_y{}^2/2 + \tilde{\mathbf{W}}_y{}^{\mathbf{T}}\tilde{\mathbf{W}}_y/2r_{Wy} + \tilde{c}_y{}^T\tilde{c}_y/2r_{cy} \\ &+ \tilde{\omega}_y{}^T\tilde{\omega}_y/2r_{\omega y} + \tilde{g}_{y\max}{}^2/2r_{gy} \end{aligned} \tag{23}$$

where the adaptive rates r_{cy} $r_{\omega y}$, r_{Wy} and r_{gy} are real and positive. Differentiating the Lyapunov function V_3 yields

$$\begin{aligned} \dot{V}_1 &\le -B_6(k_2|s_y| + k_2 s_y{}^2) + \tilde{W}_y{}^T\left(B_6\hat{\varphi}_y s_y - \dot{\hat{W}}_y/r_{Wy}\right) \\ &+ \tilde{c}_y{}^T(A_y{}^T\hat{W}_y B_6 s_y - \dot{\hat{c}}_y/r_{cy}) + \tilde{\omega}_y{}^T(B_y{}^T\hat{W}_y B_6 s_y - \dot{\hat{\omega}}_y/r_{\omega y}) \\ &+ \tilde{g}_{y\max}(B_6|s_y| - \dot{\hat{g}}_{y\max}/r_{gy}) \end{aligned} \tag{24}$$

If the following parameter adaptation rules are chosen by

$$\begin{aligned} &\dot{\hat{W}}_y = r_{Wy}\hat{\varphi}_y B_6 s_y, \dot{\hat{c}}_y = r_{cy}A_y{}^T\hat{W}_y B_6 s_y \\ &\dot{\hat{\omega}}_y = r_{\omega y}B_y{}^T\hat{W}_y B_6 s_y, \dot{\hat{g}}_{y\max} = r_{gy}B_6|s_y| \end{aligned} \tag{25}$$

Then $\dot{V}_1$ becomes $\dot{V}_1 \le -B_6(k_2|s_y| + k_2 s_y{}^2) \le 0$ which implies $\theta_y \to 0$ as $t \to \infty$ in finite time. The following summarizes the result.

Theorem 3-1 : Consider the subsystem (8) with the proposed direct FWNN yaw motion control law (13) with the parameter updating laws(25). Then $\theta_y \to 0$ in finite time.

IV.FWNN SPEED CONTROLLER DESIGN

As Fig. 1 shows, the ETWRV mobile platform has a tilt angle while starting or moving with resistance. The control objective of the sliding-mode controller is to find a speed tracking control law such that the speed of the platform tracks the linear velocity command at the flat terrain without errors, and the inclination of the platform is maintained at zero simultaneously. Keep in mind that speed command can be a function of time. In the section, this proposed controller is derived based on the well-known sliding-mode technique.

In the sequel, a sliding-mode control law is established according to the decoupled 4-state state equation(7). The control objective is to develop a sliding-mode control law C_θ , such that

$$\begin{cases} v \to v^* \\ \theta_p \to 0 \end{cases} \quad \text{as } t \to \infty \tag{26}$$

To synthesize the controller, one defines the two error scalars by $\theta_e = \theta_p$ and $v_e = v - v^*$ whose time derivatives are given by $\dot{\theta}_e = \omega_p$ and $\dot{v}_e = \dot{v} - \dot{v}^*$, respectively. Considering ω_p as a virtual control by letting $\omega_p = -k_{p2}\theta_e$, one obtains

$$\dot{\theta}_e = -k_{p2}\theta_e \ ,\ \theta_e \to 0 \text{ as } t \to \infty,\ k_{p2} > 0 \tag{27}$$

Moreover, the backstepping error for θ_e is defined as follows:

$$\eta_1 = \omega_p + k_{p2}\theta_p \tag{28}$$

To formulate the aggregate sliding-mode controller in [13], the two first-layer sliding surfaces are proposed by

$$S_1 = \eta_1\ ,\quad S_2 = \eta_2 = v_e \tag{29}$$

Then the second-layer sliding surface is written by

$$S = r_1 S_1 + r_2 S_2 = r_1\eta_1 + r_2\eta_2, r_1 \in R, r_2 \in R \tag{30}$$

To construct the aggregate sliding-mode control law [12] such that $S, S_1, S_2 \to 0$ as $t \to \infty$, one takes the time derivatives of the second-layer sliding surface to be zero

$$\begin{aligned} \dot{S} &= r_1\dot{S}_1 + r_2\dot{S}_2 = r_1\dot{\eta}_1 + r_2\dot{\eta}_2 \\ &= (r_1 A_{43} + r_2 A_{23})\sin\theta_p + (r_1 f_4 + r_2 f_2) + r_1 k_{p2}\omega_p + r_2 A_{22}v - r_2\dot{v}^* \\ &(r_1 B_4 + r_2 B_2)C_\theta \end{aligned} \tag{31}$$

which leads to the subsequent sliding-mode control law

$$C_\theta = f + [K_3|\dot{v}^*| + K_4]\mathrm{sgn}(S) \tag{32}$$

where $\Delta = r_1 B_4 + r_2 B_2 < 0$; $K_3 \ge |r_2/\Delta|$; $K_4 > 0$;

$$f=-(\frac{(r_2A_{23}+r_1A_{43})\sin\theta_p+(r_1f_4+r_2f_2)+r_1k_{p2}\omega_p+r_2A_{22}v}{\Delta}).$$

To show that $S\to 0$ as $t\to\infty$, we propose the Lyapunov function $V_2=S^2/2$ whose time derivative is expressed by

$$\dot{V}_2\le\Delta|S|[(K_3-|r_2/\Delta|)|\dot{v}^*|+K_4\Delta|S|\le K_4\Delta|S|<0 \quad (33)$$

Since $\dot{V}_2$ is negative-definite, it is easy to show that S approaches zero in finite time. From the main result present in [17], it follows that $S,S_1,S_2\to 0$ as $t\to\infty$.

However, in (34), there are two parameters and the equivalent control to be calculated by designers, in order to achieve satisfactory control performance. To circumvent this difficulty, it is good to propose the following adaptive FWNN-based control law

$$C_\theta=\hat{f}-\hat{g}_p\,\mathrm{sgn}(\Delta S)+K_5\,\mathrm{sgn}(S)+K_6S,\hat{g}_p\ge g_{p\max},K_5>0,K_6>0 \quad (34)$$

where $\hat{f}$ is the estimate of f using the FWNN proposed in Section II.B, namely that

$$f=W_p^{*T}\varphi^*_p+\varepsilon_p^*=[W_{p1}^*\cdots W_{pn}^*][\varphi^*_{p1}\quad\cdots\quad\varphi^*_{pn}]^{\mathrm{T}}+\varepsilon_p^* \quad (35)$$

where

$$\varphi^*_{pi}=\left\{1-\left(\theta_p-c^*_{1pi}\right)^2\omega^{*2}_{1pi}\right\}\left\{1-\left(\omega_p-c^*_{2pi}\right)^2\omega^{*2}_{2pi}\right\}\left\{1-(v-c^*_{3i})^2\omega^{*2}_{3pi}\right\}\left\{1-(\dot{v}^*-c^*_{4i})^2\omega^{*2}_{4pi}\right\}$$
$$*\exp\left\{-\left[\left(\theta_p-c^*_{1i}\right)^2\omega^{*2}_{1pi}+\left(\omega_p-c^*_{2i}\right)^2\omega^{*2}_{2pi}+(v-c^*_{3i})^2\omega^{*2}_{3pi}+(\dot{v}^*-c^*_{4i})\omega^{*2}_{4pi}\right]\right\}$$

(36)

Furthermore, the actual output of the FWNN is

$$\hat{f}=\hat{W}_p{}^T\hat{\varphi}_p=[\hat{W}_{p1}\cdots\hat{W}_{pn}][\hat{\varphi}_{p1}\quad\cdots\quad\hat{\varphi}_{pn}]^{\mathrm{T}} \quad (37)$$

where

$$\hat{\varphi}_{pi}=\left\{1-\left(\theta_p-\hat{c}_{1pi}\right)^2\hat{\omega}_{1pi}^2\right\}\left\{1-\left(\omega_p-\hat{c}_{2pi}\right)^2\hat{\omega}_{2pi}^2\right\}\left\{1-(v-\hat{c}_{3pi})^2\hat{\omega}_{3pi}^2\right\}\left\{1-(\dot{v}^*-\hat{c}_{4pi})^2\hat{\omega}_{4pi}^2\right\}$$
$$*\exp\left\{-\left[\left(\theta_p-\hat{c}_{1pi}\right)^2\hat{\omega}_{1pi}^2+\left(\omega_p-\hat{c}_{2pi}\right)^2\hat{\omega}_{2pi}^2+(v-\hat{c}_{3pi})^2\hat{\omega}_{3pi}^2+(\dot{v}^*-\hat{c}_{4pi})^2\hat{\omega}_{4pi}^2\right]\right\} \quad (38)$$

Similarly, by denoting $\tilde{W}_p=W_p^*-\hat{W}_p$, $\tilde{\varphi}_p=\varphi^*{}_p-\hat{\varphi}_p$, one obtains

$$f=\hat{W}_p{}^T\hat{\varphi}_p+\hat{W}_p{}^T(\bar{C}\tilde{c}_p+\bar{D}\tilde{\omega}_p)+\tilde{W}_p{}^T\hat{\varphi}_p+\varepsilon_p \quad (39)$$

where $\varepsilon_p=\hat{W}_p{}^Th+\tilde{W}_p{}^T\tilde{\varphi}_p+\varepsilon^*_p\tilde{\varphi}_p$ and ε_p is assumed to satisfy $|\varepsilon_p|<g_{p\max}$. Substituting the adaptive control law (34) into (31) yields

$$\begin{aligned}\dot{S}&=\Delta(\hat{f}-f-\hat{g}\,\mathrm{sgn}(\Delta S)+K_5\,\mathrm{sgn}(S)+K_6S)\\&=\Delta([-\hat{W}_p{}^T(\bar{C}\tilde{c}_p+\bar{D}\tilde{\omega}_p)-\tilde{W}_p{}^T\hat{\varphi}_p-\varepsilon_p]-\hat{g}_p\,\mathrm{sgn}(\Delta S)+K_5\,\mathrm{sgn}(S)+K_6S)\end{aligned} \quad (40)$$

and

$$\begin{aligned}&d\left(S^2/2\right)/dt=S\dot{S}\\&=\Delta S[-\hat{W}_p{}^T(\bar{C}\tilde{c}_p+\bar{D}\tilde{\omega}_p)-\tilde{W}_p{}^T\hat{\varphi}_p-\varepsilon_p]-\hat{g}_p|\Delta S|+\Delta K_5|S|+K_6\Delta S^2\\&\le\Delta(S[-\hat{W}_p{}^T(\bar{C}\tilde{c}_p+\bar{D}\tilde{\omega}_p)-\tilde{W}_p{}^T\hat{\varphi}_p]+[g_{p\max}-\hat{g}_p]|\Delta S|)+\Delta K_5|S|+K_6\Delta S^2\\&=\Delta S[-\hat{W}_p{}^T(\bar{C}\tilde{c}_p+\bar{D}\tilde{\omega}_p)-\tilde{W}_p{}^T\hat{\varphi}_p]+\tilde{g}_p|\Delta S|+\Delta K_5|S|+K_6\Delta S^2\end{aligned}$$

(41)

Moreover, the subsequent Lyapunov function is employed to find the parameter updating laws of $\dot{\hat{W}}_p$, $\dot{\hat{c}}_p$, $\dot{\hat{\omega}}_p$, and $\dot{\hat{g}}_p$.

$$\begin{aligned}&V_2=S^2/2+\hat{W}_p{}^T\tilde{W}_p/2r_W+\tilde{c}_p{}^T\tilde{c}_p/2r_c\\&+\tilde{\omega}_p{}^T\tilde{\omega}_p/2r_\omega+\tilde{g}_p{}^2/2r_g\end{aligned} \quad (42)$$

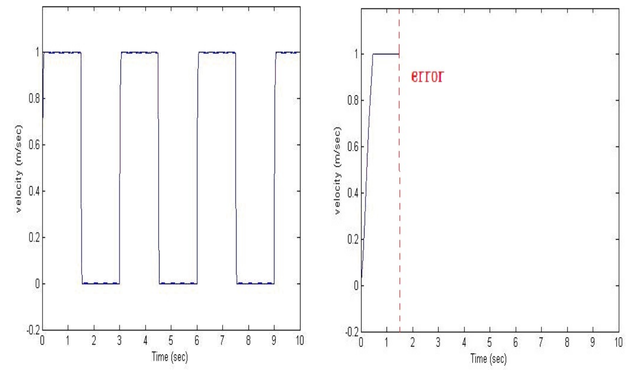

(a) (b)

Fig.3. Simulations of the speed tracking using (a) FWNN; (b)FBFN [12].

where the adaptive rates r_c, r_ω, r_W and r_g are real and positive. Differentiating the Lyapunov function V_5 yields

$$\begin{aligned}&\dot{V}_2\le\Delta K_4|S|+\hat{W}_p{}^T\left(-\hat{\varphi}_p\Delta S-\dot{\hat{W}}_p/r_W\right)+\tilde{c}_p{}^T(-\bar{C}^T\hat{W}_p\Delta S-\dot{\hat{c}}_p/r_c)\\&+\tilde{\omega}_p{}^T(-\bar{D}^T\hat{W}_p\Delta S-\dot{\hat{\omega}}_p/r_\omega)+\tilde{g}_p(|\Delta S|-\dot{\hat{g}}_p/r_g)\end{aligned} \quad (43)$$

If the following parameter adaptation rules are chosen by

$$\begin{aligned}&\dot{\hat{W}}_p=-r_W\hat{\varphi}_p\Delta S,\dot{\hat{c}}_p=-r_c\bar{C}^T\hat{W}_p\Delta S\\&\dot{\hat{\omega}}_p=-r_\omega\bar{D}^T\hat{W}_p\Delta S,\dot{\hat{g}}_p=r_g|\Delta S|\end{aligned} \quad (44)$$

Then $\dot{V}_2$ becomes $\dot{V}_2=\Delta K_5|S|+K_6\Delta S^2\le 0$ which implies $S,S_1,S_2\to 0$ as $t\to\infty$ i.e., $\theta_p\to 0$, $v\to v^*$ as $t\to\infty$. The following summarizes the result.

Theorem 4-1: Consider the subsystem (7) with the proposed direct adaptive FWNN posture and speed control law (34) with the parameter updating laws(44). Then $\theta_p\to 0$, $v\to v^*$ in finite time.

V. SIMULATIONS AND DISCUSSION

A. Direct Adaptive FWNN Posture and Speed Control

This subsection is devoted to describing simulation results of the proposed intelligent adaptive FWNN balancing and speed control method for the ETWRV. Table I lists the vehicle parameters used for simulations, where the driver is assumed to carry an extra load of 20kgw. A 4-input FWNN with 5-node hidden layer is adopted to perform on-line learning of the nonlinear term f. Other relevant parameters used for simulations are: $f_2=f_4=0.5\mathrm{N}$, $r_1=0.01$,

$r_2 = -15$, $k_{p2} = 5$, $K_5 = 5$, $K_6 = 10$, $r_W = 0.01$, $r_c = 0.01$, $r_\omega = 0.01$, $r_g = 0.01$, and the reference speed command is a square wave with an amplitude of 0.8 and a duty cycle of 50%. The initial title angle of the ETWRV was set by -3.8 degrees, and all initial values of the updating parameters are assigned by small random values. Fig.3 depicts the time responses of speed and tilt angle of the ETWRV. As shown in Fig.3, the proposed controller track the reference speed commands without errors, whereas the controller in [12] cannot follow such commands due to the program error at 1.5 seconds. The results in Fig.3 reveal that the proposed speed controller is capable of achieving speed tracking and maintaining posture at origin, and outperforms the FBFN-based controller in [12].

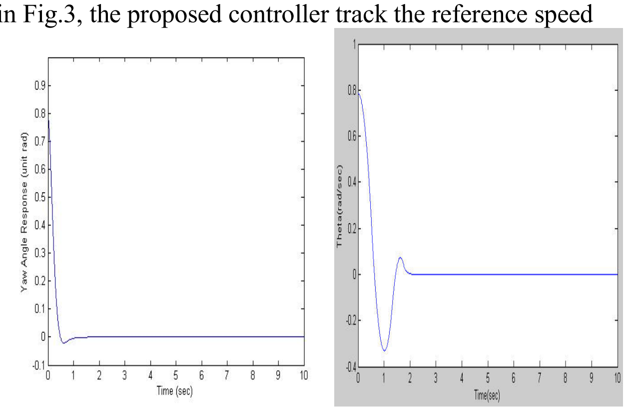

(a) (b)

Fig.4. Simulations of the yaw control using (a) FWNN; (b)FBFN [12].

B. Direct Adaptive FWNN Yaw Motion Control

This subsection conducts one simulation to examine the effectiveness of the proposed adaptive FWNN yaw motion controller. Similarly, an two-input FWNN with 5-node hidden layer is adopted to perform on-line learning of nonlinear term $\bar{\bar{f}}_6$, and the relevant parameters used for simulations are set as follows; $f_6 = 0.5$N, $K_y = 5$, $K_1 = 0$, $K_2 = 40$, $r_{Wy} = 0.01$, $r_{cy} = 0.01$, $r_{\omega y} = 0.01$, $r_{gy} = 0.01$.The ETWRV was assumed to get started at the initial tilt angle $\theta_y(0) = \pi/4$ rads. Fig. 4 presents the comparative simulations of the proposed yaw motion controller in comparison with the existing FBFN-based controller in [12] for the ETWRV. The result in Fig. 4 reveals that the proposed controller outperformed the controller in [12].

VI. CONCLUSIONS

This paper has presented a direct adaptive FWNN motion controller, composed of both speed and yaw tracking controllers, for a two-wheeled robotic vehicle with unknown parameters and uncertainties. With the decomposition of the system into two subsystems: yaw motion and mobile inverted pendulum, two direct adaptive FWNN controllers have been synthesized to respectively achieve posture and speed control and yaw motion control of the vehicle. Through simulations, both proposed controllers have been shown useful and effective in providing appropriate control actions to steer the vehicle, and they outperform the two existing FBFN-based controllers in [12]. An important topic for future research will be to conduct several experiments to examine their effectiveness of both controllers.

ACKNOWLEDGEMENTS

The authors gratefully acknowledge financial support from the National Science Council, Taiwan, R.O.C., under grant contract NSC 101-2218-E-005-046-MY2.

REFERENCES

[1]. http://www.segway.com/en-v/

[2]. http://www.tf1.fr/auto-moto/actualite/segway-general-motors-puma-vehicule-citadin-ecologique-4388637.html, July, 2011.

[3]. C. C. Tsai, H. C. Huang, S. C. Lin," Adaptive Neural Network Control of a Self-balancing Two-wheeled Scooter," *IEEE Transactions on Industrial Electronics*, vol. 57, no. 4, April 2010.

[4]. K. Pathak, J. Franch, and S. K. Agrawal, **"**Velocity and position control of a wheeled inverted pendulum by partial feedback linearization," *IEEE Trans. Robotics and Automation,* vol.21, no.3, pp.505-513, Jun. 2005.

[5]. R. O. Ambrose, R. T. Savely, S. M Goza, P. Strawser, M. A. Diftler, I.Spain, and N. Radford, "Mobile manipulation using NASA's robonaut, "*IEEE Conf. on Robotics and Automations*, pp. 2104-2109, 2004.

[6]. S. H. Jeong, T. Takahashi, "Wheeled Inverted Pendulum Type Assistant Robot : Inverted Mobile, and Sitting Motion", *IEEE/RSJ International Conference on Intelligent Robots and Systems*, pp. 1932-1937, 2007.

[7]. S. J. Lee and S. Jung, "Stabilization of a two wheeled mobile robot system under external force", *URAI,* pp. 225-228, 2010.

[8]. P. K. W. Abeygunawardhana and T. Murakami, "Vibration suppression of two-wheel mobile manipulator using resonance-ratio-control-based nullspace control", *IEEE Trans. on Industrial Electronics*, vol.57, no.12, pp.4137-4145, 2010..

[9]. C. K. Lin, S. D.Wang, "Robust self-tuning rotated fuzzy basis function controller for robot arms," *Control Theory and Applications, IEE Proceedings***,** vol.144, no.4, pp.293-298, July 1997.

[10]. Z. Huaguang, L. Cai, B. Zeungnam , "A fuzzy basis function vector-based multivariable adaptive controller for nonlinear systems." *IEEE Transactions on Systems, Man, and Cybernetics, Part B,* vol. 30 no.1, pp.210-217, Feb. 2000.

[11]. C. K. Lin, "Adaptive critic autopilot design of Bank-to-turn missiles using fuzzy basis function networks," *IEEE Transactions on Systems, Man, and Cybernetics, Part B,* vol. 35 no.2, pp.197-207, April 2005.

[12]. C. C. Tsai, S. C. Lin and B. C. Lin, "Intelligent Adaptive Motion Control Using Fuzzy Basis Function Networks for Self-Balancing Two-Wheeled Transporters," in *Proc. of 2010 IEEE International Conference on Fuzzy Systems*, Baecelona, Spain, 18-23 July 2010, pp.1-6, 2010.

[13]. D.W.C. Ho, P.A. Zhang and J. Xu, "Fuzzy wavelet networks for function learning," *IEEE Trans. on Fuzzy Systems*, vol. 9, no.1, pp.200-211, Feb. 2001.

[14]. C.K. Lin, "Nonsingular terminal sliding mode control of robot manipulators using fuzzy wavelet networks," *IEEE Trans. on Fuzzy Systems*, vol. 14, no.6, pp.849-859, Dec. 2006.

[15]. C. C. Tsai, and H.-L. Wu, "Nonsingular Terminal Sliding Control Using Fuzzy Wavelet Networks for Mecanum Wheeled Omni-directional Vehicles," *Proc. of 2010 IEEE International Conference on Fuzzy Systems*, Barcelona, Spain, 18-23 July 2010.

[16]. F. Grasser, A.D. Arrigo, and S. Colombi, "JOE: A Mobile, Inverted Pendulum," *IEEE Trans. Industrial Electronics,* vol.49, no.1, pp.107-114, Feb. 2002.

[17]. W. Wang, X. D. Liu, J. Q. Yi. "Structure design of two types of sliding-mode controllers for a class of under-actuated mechanical systems," *IET Control Theory and Applications,* vol. 1, no 1, pp. 163-172, 2007.